An inexpensive arbitrary waveform neurostimulator for the selective activation of neurons in retinal prosthesis

P. Jimenez-Fernandez[1], H. Guzman-Miranda[1], A. Barriga-Rivera[2,3]

[1] Department of Electronic Engineering, Universidad de Sevilla, Sevilla, Spain, hguzman@us.es

[2] Department of Applied Physics III, Universidad de Sevilla, Sevilla, Spain, abrivera@us.es

[3] School of Biomedical Engineering, University of Sydney, Sydney, Australia, alejandro.barriga-rivera@sydney.edu.au

Abstract

This contribution presents a two-channel inexpensive arbitrary waveform neurostimulator based on a Raspberry Pi microcomputer platform and a Howland voltage-to-current converter. The system has been designed to enable the delivery of common stimulation strategies used in visual prosthesis research.

1. Introduction

Retinal electrostimulation has enabled the restoration of visual sensations in patients suffering from retinal degeneration diseases [1, 2]. By delivering current pulses, it is possible to bypass the photoreceptors and activate the surviving neurons in the retina. These electrical pulses will be eventually converted into artificially-generated visual information in the form of sequences of action potentials.

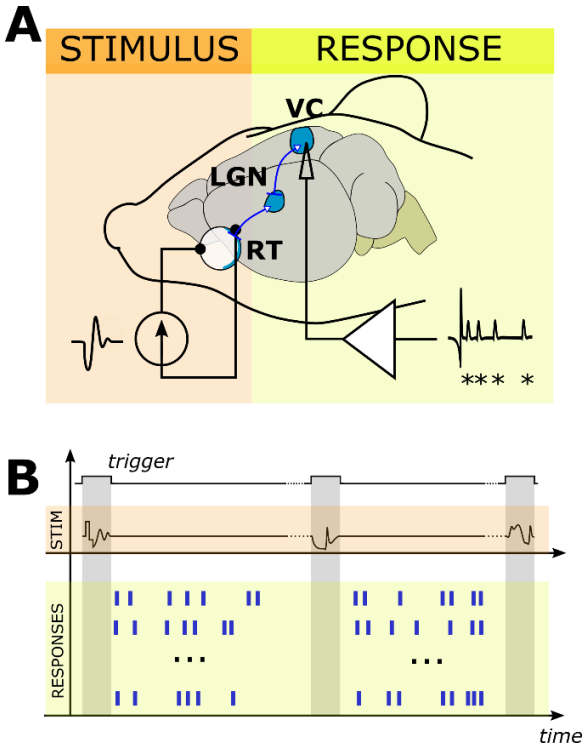

Figure 1. *Schematic showing the typical experimental setup used in in vivo visual prosthesis research. Panel A illustrates the delivery of an arbitrary current waveform to the retina (RT) of an experimental subject. Neural responses thus generated travel to the lateral geniculate nucleous (LGN) and, subsequently, to the visual cortex (VC). An array of recoding electrodes is interfaced to a neural amplifier used to obtain the neural responses. Panel B shows an schematic of the occurrence of stimuli and responses governed by a trigger signal.*

This information, referred to here as 'neural message', propagates downstream to higher visual centres to ultimately elicit a visual sensation. There are, however, two important limitations in this process [3]: (1) the neural messages thus generated differ from those in physiological vision, and (2) the brain has undergone an important neural remodelling that may alter the way visual information is processed.

The visual prosthesis research community continues to investigate new ways of producing more physiological neural messages [4]. While classical constant-current pulses and current-steering techniques can allow for fine spatial [5, 6] and in-depth [7] recruitment of retinal neurons, kilohertz pulse trains have demonstrated, *in vitro* and *in silico*, the potential of non-conventional current waveforms to produce the selective activation of different retinal pathways [8, 9]. To date, these stimulation strategies have relied on the use of amplitude-modulated high-frequency pulse trains, as most of the neural stimulators available rely on the generation of constant-current pulses. Here we report the design of an inexpensive arbitrary waveform neural stimulator for research applications in visual prosthesis.

2. Description of the system.

Visual prosthesis research requires complex and expensive setups [10]. These experimental setups typically include a multi-channel neural recording system and a neurostimulator, both connected to deliver the targeted stimulation strategy and to record the neural activity thus elicited. While communication and synchronisation of these subsystems can be achieved in many ways, trigger signals are normally employed to indicate the delivery of a given stimulus, as shown in figure 1. This signal can be generated by the recording subsystem, by the stimulator, or by an external trigger source.

The design of the neural stimulator presented here was conceived to deliver arbitrary current waveforms with frequency components up to 30 kHz to ensure the kilohertz frequencies previously described in preferential activation experiments was attainable [9]. Secondly, given the current levels previously reported to drive ganged [11] or large electrodes [12, 13], the stimulator was design to allow for the delivery of current levels of up to ±3 mA. Note the expected impedance value ranges from 100 Ω to approximately 10 kΩ. And thirdly, a neural stimulator designed for research must allow for different experimental

ISBN: 978-84-17853-76-1

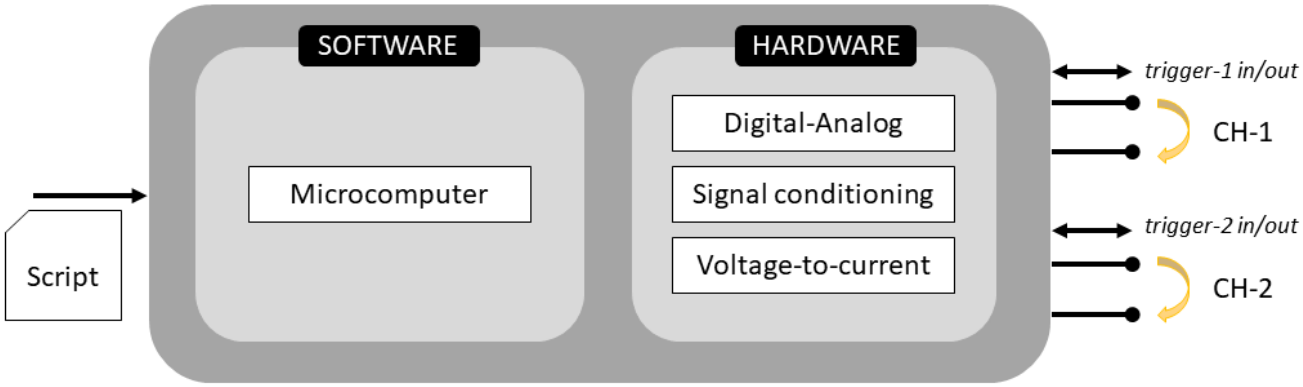

Figure 2. *Conceptual diagram illustrating the subsystems of the two-channel arbitrary neural stimulator. It comprises a software subsystem running on a microcomputer, and a hardware subsystem for the generation of the current waveforms (digital-to-analog conversion, signal conditioning, and voltage-to-current conversion). A script file contains a set of instructions for the delivery of a series of stimuli and the control of the trigger signals of each channel (CH-1 and CH-2).*

configurations. For that purpose, we used a microcomputer system to easily program (1) the current waveforms to be delivered, (2) the trigger regimes to be used, and (3) the workflow of the experiments.

3. Logical view

The logical view, adapted from the 4+1 view model reported by Krutchen [14], provides a picture of the different constituents of the system. The two-channel arbitrary neural stimulator described herein includes two main subsystems: a hardware subsystem and a software subsystem. The neurostimulator software runs on a Raspberry Pi (RPi) 3 Model B (Raspberry Pi Foundation, Cambridge, UK) microcomputer running Raspbian operating system. This software receives a script file containing a set of instructions via USB serial communications. These instructions codify the samples of each arbitrary waveform to be delivered as well as the inter-stimulus delays and the trigger configurations thus established. Said microcomputer is interfaced to a custom hardware subsystem designed for the generation of analog signals, and for the management of the trigger signals required to deliver the target stimulation regimen, as shown in figure 2. The output of the stimulator is to be connected to the stimulation electrodes. Shorting of the electrodes is controlled by the trigger signal. This trigger signal can be either internally generated by the neurostimulator, or received from an external device.

4. Physical view

The physical view describes the hardware components of the neurostimulator. The RPi 3 microcomputer was chosen in this neurostimulator as it is broadly used in academic applications due to the availability and the maturity of the system. On the one hand, the microcomputer provides the physical substrate for the software subsystem. On the other hand, the hardware subsystem referred to in the previous section required further description from a physical viewpoint. These subsystems were implemented as electronic circuits on a custom printed circuit board (PCB).

4.1. Power supply

The voltage compliance limits in this system have to allow for driving 10-kΩ impedances with currents of ±3 mA. To ensure this requirement is met, we connected three TMA0515D (Traco Power, Sihlbruggstrasse, Switzerland) isolated DC-DC converters in series to provide ±45 V. Additionally, we also included a L7805CV (STMicroelectronics, Geneva, Switzerland) voltage regulator to provide a 5-V supply to the signal conditioning circuits, as shown in figure 3.

4.2. Digital-analog conversion (DAC)

The RPi microcomputer generates digital data to codify the samples of the current waveforms at approximately 166 kHz. These data are transmitted *via* I^2C protocol to a MCP4725 (Microchip Technologies, Chandle, USA) digital-to-analog module using 12 bits per sample.

4.3. Signal conditioning

Signal conditioning here includes a low-pass filtering stage, a voltage level adjustment and signal amplification. An RC low-pass filter was implemented to provide a 3-dB cut-off frequency of 160 kHz. Subsequently, voltage signal was linearly scale to adjust the 0-to-5 voltage range provided by the DAC to a symmetrical range between -3 and 3 V. For that purpose, a TL082CP (Texas Instruments, Dallas, USA) operational amplifier was topologically configured as a summing amplifier to implement equation (1), where V_{DAC} represents the voltage value provided after low pass filtering, and V_{adjust} is the adjusted voltage output.

$$V_{adjusted} = \frac{5}{6} V_{DAC} - 3 \quad (1)$$

4.4. Signal isolation.

The voltage signal thus adjusted needs to be electrically isolated from the common ground. To provide this isolated grounding, an isolation amplifier ISO124-P (Texas Instruments, Dallas, USA) was employed. The gain of this stage was 1, and consequently, it is referred to as an isolation buffer in figure 2.

ISBN: 978-84-17853-76-1

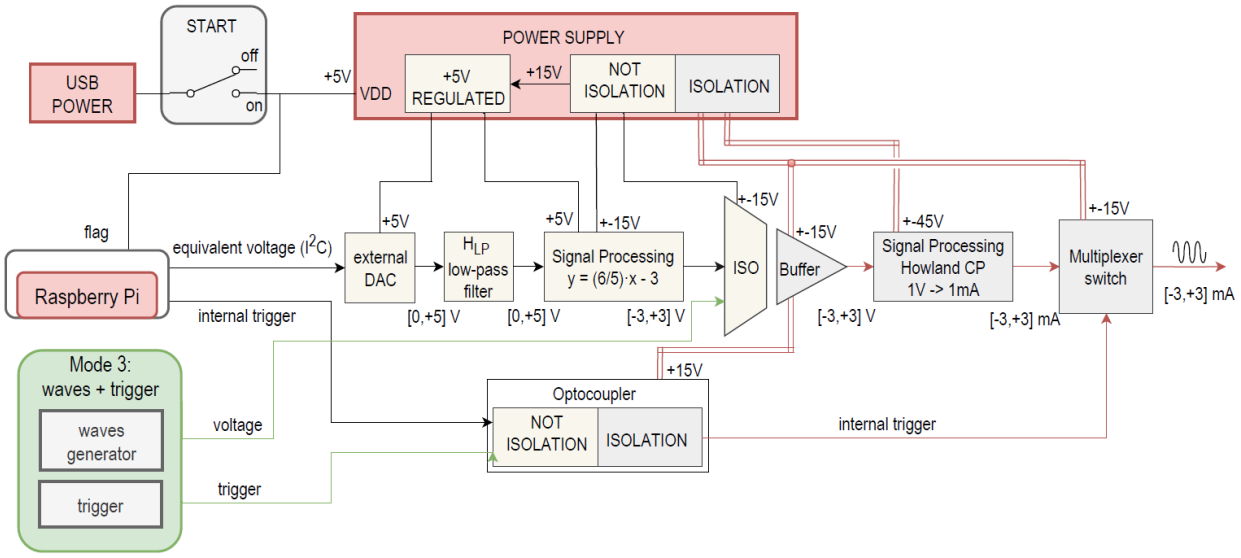

Figure 2. *Block diagram of the neurostimulator circuitry. The electronics are powered using the 5-V supply provided by the Raspberry Pi board. The power supply unit provides all required voltages to the other subsystems. The analog-to-digital (DAC) converter is driven by the Raspberry Pi using the I²C communication protocol. The voltage waveform thus generated is low-pass filtered and linearly scaled between +3 and -3 V, and subsequently isolated from the common ground using an isolation amplifier (ISO). It is then converted to a current waveform using a Howland voltage-to-current converter. Shorting of the electrodes is achieved by an analog multiplexer digitally controlled by an electrically isolated trigger signal. Additionally, an external arbitrary function generator can be wired to the single processing subsystems to generate other types of current waveforms (functioning mode 3).*

4.5. Voltage-to-current conversion.

Neural stimulation is normally achieved using current-controlled devices, as it allows for controlling the amount of charge delivered and recovered during the stimulus. Thus, the arbitrary voltage waveforms obtained are to be converted into current waveforms. For that purpose, an improved Howland current source [15] was implemented using a high-voltage precision operational amplifier ADA4700 (Analog Devices, Wilmington, USA) power at ± 45 V to provide a wide voltage compliance range as shown in figure 3. Note the conversion rate achieved with this circuit was 1 mA·V^{-1}.

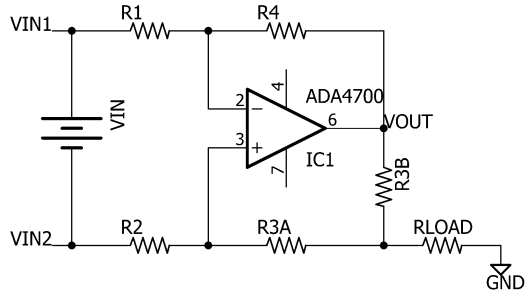

Figure 3. *Circuit diagram of the Howland current source implemented in the arbitrary neurostimulator.*

4.6. Trigger and electrode shorting.

The trigger signal, as described previously, is used to provide a time mark for the stimulus delivery. The trigger signal is also used to connect and disconnect the neurostimulator to the electrodes. On the one hand, with a high-level input voltage the output of the current source is connected to the target electrodes. On the other hand, with a low-level input voltage the terminals of the electrodes are shorted, and the output terminals of the current source are also shorted. This is achieved using a CD4053BE (Texas Instruments, Dallas, USA) digitally-controlled analog multiplexer mounted as illustrated in figure 4. The trigger signal can be internally generated (functioning mode 1), or received from an external device (functioning mode 2).

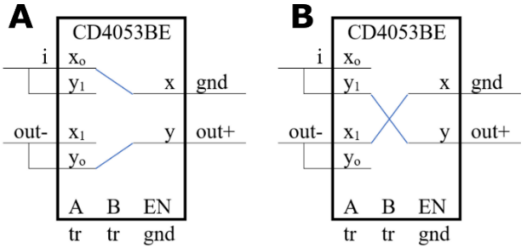

C

AB	x		y	
	x_o	x_1	y_o	y_1
low	1	-	1	-
high	-	1	-	1

Figure 4. *Connection diagram of the digitally-controlled analog multiplexor used in the arbitrary neurostimulator to allow for the shorting of the electrodes. Panel A and B illustrate the internal switching for high- and low- logic level of the trigger signal respectively. Panel C shows the electrical configuration required in terminals A and B of the CD4053BE chip.*

5. Development and process views

We have described the hardware components of the arbitrary wave for neurostimulator herein presented. However, the system needs a custom software to implement a given stimulation strategy. For that purpose, the software subsystem has been developed by combining two software elements that interact to facilitate the user experience. Hence, the development and the process view referred to in the 4+1 architecture model have been combined in this section.

ISBN: 978-84-17853-76-1

5.1. Matlab scripting.

The definition of the stimulus waveforms is carried out using a custom Matlab script. Briefly, this script generates all waveform samples required to drive the DAC and interstimulus delay times to be applied. The script, executed on a personal computer, generates a file containing said information. This file is to be transferred onto the RPi system using a USB memory stick.

5.2. Script execution.

A custom software developed in C language has been programmed to read the data file containing stimulus parameters and to drive the DAC of the neurostimulator using the I^2C communication protocol.

5.3. Communication and interaction.

As described previously, the user defines the stimulation strategy. This typically consists of a series of stimuli, defined by the waveform samples, the trigger values (ON/OFF) and the inter-stimulus time, as illustrated in figure 1. Once the user runs the Rpi software, the neuroestimulator will proceed with the delivery of the stimulation regimen programmed in the input file.

6. Experimental validation and discussion.

The neurostimulator has been tested using a 100 kΩ to ensure the system complies with strict requirements. While the neurostimulator was able to meet the current and bandwidth requirements established, a substantial ringing was observed for low-current levels, as shown in figure 5. This appears due to the low-voltage input at the entrance of the isolation buffer. This limitation can be improved by either re-scaling the gains of the signal conditioning and the voltage-to-current stages, or by using higher-end isolation buffers. Further testing is required *in vitro* and *in vivo*. In addition, while this is an experimental prototype, the channel count will need to be increased when driving multi-electrode retinal prostheses.

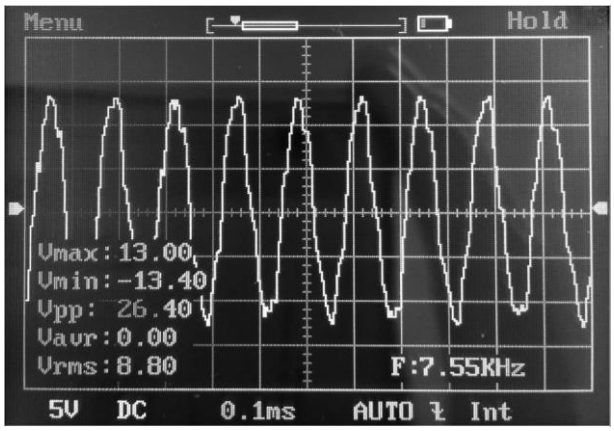

Figure 5. *Voltage waveform recorded using an isolated oscilloscope from a 100-kΩ driven by a 200-μA sinusoidal current waveform at 7.5 kHz.*

Acknowledgements

This work has been funded by grant CNS2022-135870 funded by MCIN/AEI/ 10.13039/501100011033 and by "European Union NextGenerationEU/PRTR", and supported by 'FUNDALUCE' (Foundation for Fighting Blindness). Part of this work was developed by the first author as part of final year project, submitted to the University of Seville in partial fulfilment for the requirements of his undergraduate degree.

References

[1] P. J. Allen *et al.*, "Ten year safety and stability results of a suprachoroidal retinal prosthesis," *Investigative Ophthalmology & Visual Science*, vol. 64, no. 8, pp. 3827-3827, 2023.

[2] L. N. Ayton *et al.*, "An update on retinal prostheses," *Clinical Neurophysiology*, vol. 131, no. 6, pp. 1383-1398, 2020.

[3] D. Caravaca-Rodriguez, S. P. Gaytan, G. J. Suaning, and A. Barriga-Rivera, "Implications of neural plasticity in retinal prosthesis," *Investigative Ophthalmology & Visual Science*, vol. 63, no. 11, pp. 11-11, 2022.

[4] W. Tong, H. Meffin, D. J. Garrett, and M. R. Ibbotson, "Stimulation strategies for improving the resolution of retinal prostheses," *Frontiers in neuroscience*, vol. 14, p. 262, 2020.

[5] A. Barriga-Rivera, J. W. Morley, N. H. Lovell, and G. J. Suaning, "Cortical responses following simultaneous and sequential retinal neurostimulation with different return configurations," in *2016 38th Annual International Conference of the IEEE Engineering in Medicine and Biology Society (EMBC)*, 2016: IEEE, pp. 5435-5438.

[6] G. Dumm, J. B. Fallon, C. E. Williams, and M. N. Shivdasani, "Virtual electrodes by current steering in retinal prostheses," *Investigative ophthalmology & visual science*, vol. 55, no. 12, pp. 8077-8085, 2014.

[7] Z. C. Chen, B.-Y. Wang, and D. Palanker, "Real-time optimization of the current steering for visual prosthesis," in *2021 10th International IEEE/EMBS Conference on Neural Engineering (NER)*, 2021: IEEE, pp. 592-596.

[8] P. Twyford, C. Cai, and S. Fried, "Differential responses to high-frequency electrical stimulation in ON and OFF retinal ganglion cells," *Journal of neural engineering*, vol. 11, no. 2, p. 025001, 2014.

[9] T. Guo *et al.*, "Closed-loop efficient searching of optimal electrical stimulation parameters for preferential excitation of retinal ganglion cells," *Frontiers in neuroscience*, vol. 12, p. 168, 2018.

[10] A. Barriga-Rivera *et al.*, "A 4+ 1 architecture for in vivo electrophysiology visual prosthesis," *Journal of Accessibility and Design for All*, pp. 81-101, 2016.

[11] A. Barriga-Rivera *et al.*, "High-amplitude electrical stimulation can reduce elicited neuronal activity in visual prosthesis," *Scientific reports*, vol. 7, no. 1, p. 42682, 2017.

[12] A. Barriga-Rivera, T. Guo, J. W. Morley, N. H. Lovell, and G. J. Suaning, "Retinal electrostimulation in rats: activation thresholds from superior colliculus and visual cortex recordings," in *2017 39th Annual International Conference of the IEEE Engineering in Medicine and Biology Society (EMBC)*, 2017: IEEE, pp. 1166-1169.

[13] A. Barriga-Rivera, V. Tatarinoff, N. H. Lovell, J. W. Morley, and G. J. Suaning, "Long-term anesthetic protocol in rats: feasibility in electrophysiology studies in visual prosthesis," *Veterinary ophthalmology*, vol. 21, no. 3, pp. 290-297, 2018.

[14] P. B. Kruchten, "The 4+ 1 view model of architecture," *IEEE software*, vol. 12, no. 6, pp. 42-50, 1995.

[15] A. Mahnam, H. Yazdanian, and M. M. Samani, "Comprehensive study of Howland circuit with non-ideal components to design high performance current pumps," *Measurement*, vol. 82, pp. 94-104, 2016.